PCCP

PAPER

View Article Online
View Journal | View Issue

Cite this: *Phys. Chem. Chem. Phys.*, 2015, **17**, 29697

On the structure and bonding in the $B_4O_4^+$ cluster: a boron oxide analogue of the 3,5-dehydrophenyl cation with π and σ double aromaticity†

Ting Ou,[a] Wen-Juan Tian,[a] Xue-Rui You,[a] Ying-Jin Wang,[ab] Kang Wang[a] and Hua-Jin Zhai*[ac]

Received 31st July 2015,
Accepted 7th October 2015

DOI: 10.1039/c5cp04519c

www.rsc.org/pccp

Boron oxide clusters offer intriguing molecular models for the electron-deficient system, in which the boronyl (BO) group plays a key role and the interplay between the localized BO triple bond and the multicenter electron delocalization dominates the chemical bonding. Here we report the structural, electronic, and bonding properties of the $B_4O_4^+$ cationic cluster on the basis of unbiased Coalescence Kick global-minimum searches and first-principles electronic structural calculations at the B3LYP and single-point CCSD(T) levels. The $B_4O_4^+$ cluster is shown to possess a C_s (**1**, $^2A'$) global minimum. It represents the smallest boron oxide species with a hexagonal boroxol (B_3O_3) ring as the core, terminated by a boronyl group. Chemical bonding analyses reveal double (π and σ) aromaticity in C_s $B_4O_4^+$, which closely mimics that in the 3,5-dehydrophenyl cation $C_6H_3^+$ (D_{3h}, $^1A_1'$), a prototypical molecule with double aromaticity. Alternative D_{2h} (**2**, $^2B_{3g}$) and C_{2v} (**3**, $^2A_1$) isomeric structures of $B_4O_4^+$ are also analyzed, which are relevant to the global minima of B_4O_4 neutral and $B_4O_4^-$ anion, respectively. These three structural motifs vary drastically in terms of energetics upon changing the charge state, demonstrating an interesting case in which every electron counts. The calculated ionization potentials and electron affinities of the three corresponding neutral isomers are highly uneven, which underlie the conformational changes in the $B_4O_4^{+/0/-}$ series. The current work presents the smallest boron oxide species with a boroxol ring, establishes an analogy between boron oxides and the 3,5-dehydrophenyl cation, and enriches the chemistry of boron oxides and boronyls.

1. Introduction

There has been persistent research interest in boron oxides during the past 60 years, which primarily aims at the development of highly energetic boron-based propellants.[1] Renewed recent interest in this direction focuses on the electronic, structural, and chemical bonding properties of boron oxide clusters in the gas phase, where the boronyl (BO) group emerges as a new inorganic ligand.[2] Note that BO and BO^- possess a robust B≡O triple bond.[3,4] These species are isovalent to CN and CN^-/CO, respectively, which are well-known inorganic ligands, hinting opportunities to develop the chemistry of boronyls and boron oxides.[2,5–13] The geometric structures of boron oxide clusters exhibit vast diversity, which are governed by the complexity in their chemical bonding.

Boron is a prototypical electron-deficient element, leading to unique planar or quasi-planar structures for a wide range of boron clusters, B_n^- (n = 3–27, 30, 35, 36, 40),[14–19] which are in stark contrast to bulk boron and boron alloys. The bonding in planar and quasi-planar boron clusters is governed by multiple aromaticity and antiaromaticity, rendering them interesting all-boron analogues of the aromatic hydrocarbons.[20–23] Beyond the flat world of boron, the first cage-like boron clusters, D_{2d} B_{40}^-/B_{40}, were observed in 2014,[19] which are referred to routinely as all-boron fullerenes, or borospherenes. New chiral members were subsequently introduced to the borospherene family: C_3/C_2 B_{39}^-, C_1 B_{41}^+, and C_2 B_{42}^{2+}.[24,25] The bonding in borospherenes features the interwoven boron double chains

[a] *Nanocluster Laboratory, Institute of Molecular Science, Shanxi University, Taiyuan 030006, China. E-mail: hj.zhai@sxu.edu.cn*
[b] *Department of Chemistry, Xinzhou Teachers University, Xinzhou 034000, China*
[c] *State Key Laboratory of Quantum Optics and Quantum Optics Devices, Shanxi University, Taiyuan 030006, China*

† Electronic supplementary information (ESI) available: Optimized D_{2h} ($^2B_{3g}$) and C_{2v} ($^2A_1$) structures of $B_4O_4^+$ and C_{2h} (^1A_g) structure of B_4O_4 at the B3LYP/aug-cc-pVTZ level; canonical molecular orbitals (CMOs) of the quasi-linear C_{2h} isomer of $B_4O_4^+$; natural charge distributions of the global minimum and selected low-lying isomers for $B_4O_4^+$: C_s ($^2A'$), C_{2h} (^2B_u), D_{2h} ($^2B_{3g}$), and C_{2v} ($^2A_1$); and Cartesian coordinates at the B3LYP/aug-cc-pVTZ level for the four isomeric structures (C_s, C_{2h}, D_{2h}, and C_{2v}). See DOI: 10.1039/c5cp04519c

and the π plus σ double delocalization, which effectively compensates for boron's intrinsic electron-deficiency.[19] This bonding pattern differs fundamentally from that in C_{60}. Boron oxide clusters are the oxidation products of elemental boron clusters. As a consequence, boron oxide clusters are intuitively considered to be even more electron-deficient. Nonetheless, the available O 2p electrons in boron oxide clusters can greatly enrich the BB and BO interactions, leading to exotic chemical bonding. Aromaticity and antiaromaticity, boronyls, multicenter BO rings, and B *versus* O atomic ratio are some of the key factors that dominate the structure and bonding in boron oxide clusters.[2,26–29]

In an early gas-phase experimental work,[30] Doyle carried out extensive collision induced dissociation (CID) measurements on a variety of cationic boron oxide clusters, $B_mO_n^+$. Among these, the $B_4O_4^+$ cluster was observed to be unusual, whose collisional activation spectrum deviates from the general trend of boron oxides. The CID products "are consistent only with a structure containing a B–B bond".[30] Based on this observation, Doyle proposed a "speculative" linear structure for $B_4O_4^+$, as illustrated in Scheme 1. For a quarter of a century, this structure has remained untested. Our recent interest in boron oxide clusters[2] has motivated us to revisit this cluster using the modern quantum chemistry tools.

Closely relevant to the current topic, we carried out a systematic computational study lately on small boron oxide clusters, $B_3O_n^{+/0/-}$ (n = 2–4), which are shown to adopt either rhombic or open structures.[26] We also predicted the viability of boronyl boroxine, D_{3h} B_6O_6, which possesses a boroxol (B_3O_3) ring as the core with an aromatic π sextet, rendering it a boron oxide analogue of boroxine ($B_3O_3H_3$) and benzene.[27] Furthermore, we performed a joint photoelectron spectroscopy (PES) and computational study on the $B_4O_4^{0/-}$ clusters,[29] establishing the rhombic and Y-shaped global-minimum structures for B_4O_4 and $B_4O_4^-$, respectively. In this contribution, we report on the structural, electronic, and bonding properties of the cationic $B_4O_4^+$ cluster using extensive Coalescence Kick (CK)[31,32] structural searches, electronic structural calculations, and canonical molecular orbital (CMO) and adaptive natural density partitioning (AdNDP) analyses.[33] The $B_4O_4^+$ cluster is shown to possess a hexagonal C_s (**1**, $^2A'$) global minimum, which marks the exact onset of the boroxol ring in small boron oxide species (that is, the smallest boron oxide cluster with a boroxol ring). Bonding analyses reveal double (π and σ) aromaticity in C_s $B_4O_4^+$, rendering it a boron oxide analogue of the 3,5-dehydrophenyl cation $C_6H_3^+$ (D_{3h}, $^1A_1'$).[34] The hexagonal C_s $B_4O_4^+$ global minimum is markedly different from the 1988 linear structure (Scheme 1), as well as the rhombic structure of B_4O_4 and the Y-shaped one of $B_4O_4^-$.[29] The current C_s $B_4O_4^+$ global-minimum structure also helps reinterpret the early experimental collisional activation spectrum.[30]

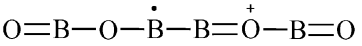

Scheme 1 A speculative structure for the $B_4O_4^+$ cationic cluster, proposed by Doyle[30] in 1988.

2. Computational methods

Global-minimum searches for the cationic $B_4O_4^+$ cluster were carried out *via* unbiased CK searches[31,32] using the hybrid B3LYP method with the small basis set of 3-21G. The structural searches were also aided with manual structural constructions. A total of 2000 stationary points on the potential energy surface were probed in the CK searches. Low-lying candidate structures were then fully re-optimized at the B3LYP/aug-cc-pVTZ level,[35] which has been established lately to be an appropriate method for the boron oxide systems in extensive experimental and computational studies.[2] Frequency calculations were performed to ensure that all reported structures are true minima. Furthermore, single-point CCSD(T) calculations[36–38] were done at the B3LYP/aug-cc-pVTZ geometries to benchmark the relative energies for the top low-lying structures. Chemical bonding was elucidated *via* the AdNDP and CMO analyses. Natural bond orbital (NBO) analysis[39] was performed to obtain the natural atomic charges. The AdNDP calculations were accomplished using the AdNDP program[33] and all other calculations were performed using the Gaussian 09 package.[40]

3. Results

3.1. Global-minimum structure

While one can always be cautious about the capability of modern quantum chemistry in identifying the true global minimum of a molecular system, we are quite confident in the current case for two reasons. First, $B_4O_4^+$ is a relatively small system and one is expected to find its global-minimum structure simply *via* manual structural constructions, without the need for aid from computational searches. Second, the CK algorithm[31,32] is one of the state-of-the-art and well tested methods in unbiased structural searches. We reiterate specifically that 2000 stationary points were probed on the potential energy surface in our CK searches for such a small cluster, which is a heroic effort.

The global minimum of $B_4O_4^+$, **1** (C_s, $^2A'$), is depicted in Fig. 1(a). Also shown are the bond distances at the B3LYP/aug-cc-pVTZ level. The corresponding symmetric C_{2v} structure of $B_4O_4^+$ turns out not to be a true minimum, with one imaginary frequency of 547.19i cm^{-1} at the B3LYP level. To further verify that the C_{2v} structure is a first-order saddle point, we have run a complementary PBE0/aug-cc-pVTZ calculation, which also reveals one imaginary frequency (634.15i cm^{-1}). It is thus safe to conclude that the C_s distortion of **1** is not a computational artifact. As shown in Fig. 2, the structure of **1** (C_s, $^2A'$) is clearly the global minimum of the $B_4O_4^+$ system, at both the B3LYP and single-point CCSD(T) levels of theory. It is perfectly planar, being composed of a hexagonal boroxol ring and a terminal boronyl group. The B1B2 and B2O5 distances (1.66 and 1.19 Å) are typical for single B–B and triple B≡O bonds, respectively,[41–43] consistent with the general notion that the boronyl group is a robust monovalent σ radical.[2]

The six B–O distances within the boroxol ring in **1** are uneven (Fig. 1(a)), suggesting obvious structural distortions. The two intermediate distances (1.34–1.38 Å) are similar to

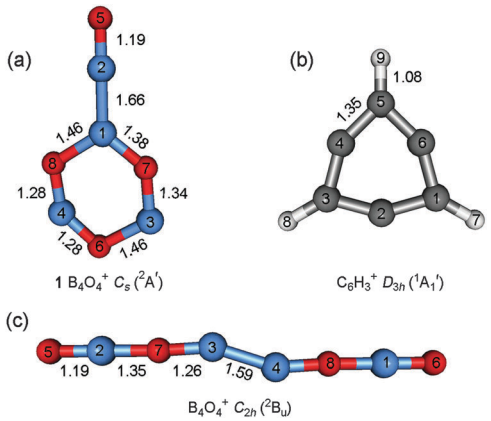

Fig. 1 Optimized cluster structures at the B3LYP/aug-cc-pVTZ level. (a) Global-minimum structure **1** (C_s, $^2A'$) of $B_4O_4^+$. (b) 3,5-Dehydrophenyl cation ($C_6H_3^+$). (c) A typical quasi-linear isomeric structure of $B_4O_4^+$ on the basis of a prior proposal of 1988.[30] Atoms are labeled numerically and the bond distances are denoted in Å. The B atom is in blue, O in red, C in thick gray, and H in light gray.

those in boroxine and boronyl boroxine (1.38 Å at B3LYP/6-311+G(d,p)).[27] The two long distances (1.46 Å) appear to be close to the upper limit of a single B–O bond,[41] whereas the two short ones (1.28 Å) are markedly shorter than a typical B–O single bond and close to a B=O double bond.[26,41] Thus, the overall bonding in the boroxol ring in **1** is substantially greater than six B–O single bonds.

3.2. Selected isomeric structures

Alternative low-lying isomeric structures of $B_4O_4^+$ are shown in Fig. 2, along with their relative energies at the B3LYP and single-point CCSD(T) levels. The energetics at B3LYP and CCSD(T) are generally consistent with each other, suggesting that the global-minimum structure, **1** (C_s, $^2A'$), is reasonably well defined on the potential energy surface. Indeed, the nearest low-lying isomer is 14 and 10 kcal mol^{-1} above the global minimum at B3LYP and CCSD(T) levels, respectively. Among the higher energy isomers, we are interested in the quasi-linear C_{2h} (^2B_u), rhombic **2** (D_{2h}, $^2B_{3g}$), and Y-shaped **3**

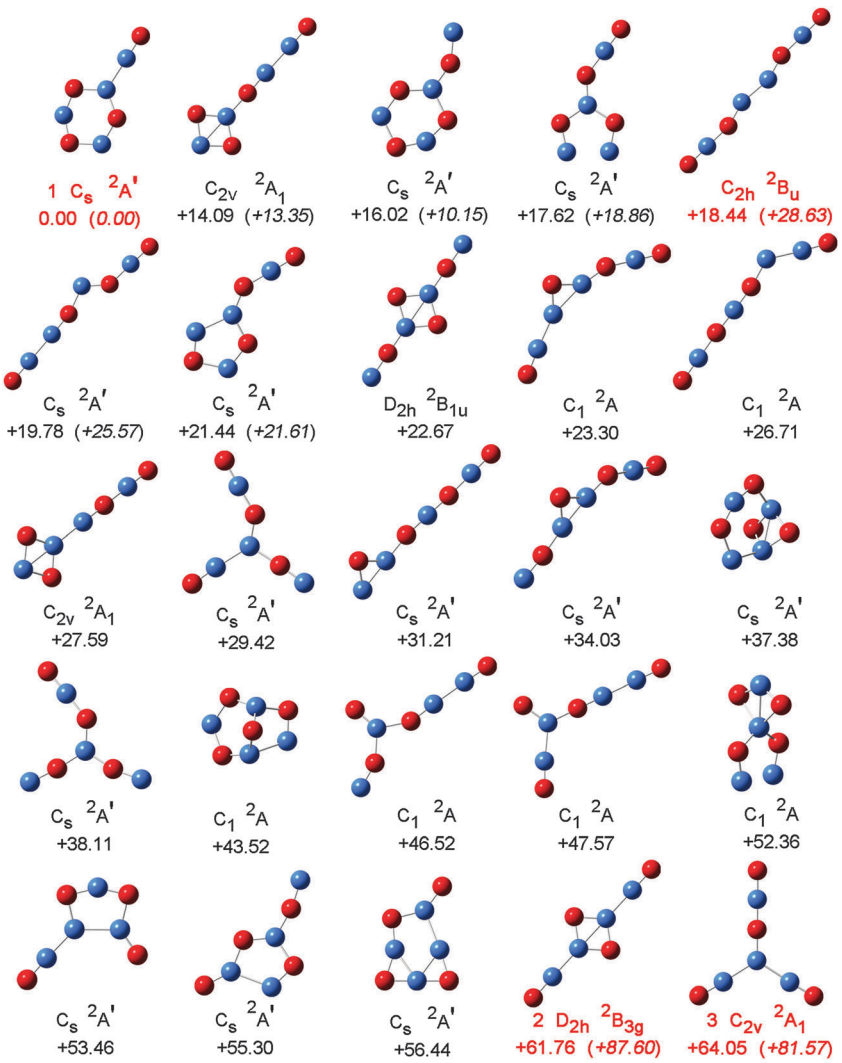

Fig. 2 Alternative optimized isomeric structures of $B_4O_4^+$ at the B3LYP/aug-cc-pVTZ level. The relative energies (in kcal mol^{-1}) are indicated at the B3LYP/aug-cc-pVTZ and the single-point CCSD(T)//B3LYP/aug-cc-pVTZ (in italic) levels. The B atom is in blue and O is in red.

(C_{2v}, $^2A_1$), which are approximately 29, 88, and 82 kcal mol^{-1} above the global minimum **1**. All the three structures are also perfectly planar.

Quasi-linear C_{2h} (^2B_u) is illustrated in Fig. 1(c). It can be considered as the fusion of two BOBO units, or four BO units. The two terminal BO groups possess bond distances of 1.19 Å and are readily assigned as boronyls.[2] The remaining two BO units have distances of 1.26 Å, which also show triple bond character but are slightly longer than typical B≡O bonds.[2,4] The B2O7 and B1O8 bonds (1.35 Å) are roughly B–O single bonds, whereas the B3B4 distance (1.59 Å) is between typical B–B single and B=B double bonds.[12,41] Note that this isomer is basically in the spirit of the "speculative" linear structure of $B_4O_4^+$, proposed initially in 1988.[30] However, the bonding details in the two structures differ substantially (Fig. 1(c) *versus* Scheme 1).

Isomer **2** (D_{2h}, $^2B_{3g}$) possesses a rhombic B_2O_2 core, attached by two terminal boronyl groups (Fig. 2). The terminal BO and BB distances (1.24 and 1.69 Å, respectively; Fig. S1 in the ESI†) are consistent with triple B≡O and single B–B bonds,[2,41] whereas the rhombic BO distances (1.40 Å) are comparable to a B–O single bond. A similar D_{2h} (^1A_g) structure was recently located as the global minimum for the B_4O_4 neutral cluster,[29] whose B≡O, B–B, and B–O distances are 1.20, 1.67, and 1.40 Å, respectively. Only minor structural differences are observed between **2** of $B_4O_4^+$ and D_{2h} (^1A_g) of B_4O_4.

The Y-shaped isomer **3** (C_{2v}, $^2A_1$) of $B_4O_4^+$ (Fig. 2 and Fig. S1 in the ESI†) are associated with the C_s ($^2A''$) global minimum of the $B_4O_4^-$ anion cluster.[29] In the latter, the terminal OBO is bent. The two terminal BO groups in **3** (1.19 Å) are boronyls. The short and long BO distances in the OBO unit (1.24 *versus* 1.29 Å) are approximately assigned as B≡O and B=O bonds, respectively.[2,41] The BO distance associated with the central B atom (1.34 Å) is a B–O single bond. The two BB distances in **3** (1.70 Å) are slightly elongated with respect to the B–B single bond in **1** (1.66 Å; Fig. 1(a)), consistent with the fact that only 3 electrons are available for the two BB bonds in **3** (due to the positive charge). The formal BB bond order is 0.75. Going from **3** of $B_4O_4^+$ to the C_s ($^2A''$) global minimum of $B_4O_4^-$, one observes bond distance changes associated with the center B atom: the B–O and B–B bonds are 1.46 and 1.64 Å, respectively, in the latter structure.[29]

4. Discussion

4.1. Hexagonal C_s $B_4O_4^+$ cluster: the genesis of the boroxol ring in boron oxides

Bulk boron oxides are amorphous and difficult to crystallize, whose structures have remained controversial in the literature. However, it is generally believed that the boroxol ring constitutes a large fraction of them, probably up to 75%.[44] Furthermore, it has been speculated that the high temperature B_2O_3 liquids are also networked by the boroxol rings, terminated with boronyl groups.[45] It is thus desirable to characterize the intrinsic stability and bonding of the boroxol ring in gas-phase boron oxide clusters. In particular, what is the smallest, free-standing boron oxide cluster that can support a boroxol ring? In other words, how many B/O atoms are needed at the minimum in order to self-assemble into a chemical species that contains a boroxol ring? The present results offer a definite answer.

The lower bound to explore the onset of the boroxol ring is the $B_3O_n^{-/0/+}$ ($n \geq 3$) cluster. However, our recent systematic computational searches on a series of $B_3O_n^{-/0/+}$ (n = 2–4) clusters concluded that the boroxol ring is not present in them, and only three out of these nine species have a rhombic B_2O_2 ring.[26] As an upper bound, the boronyl boroxine (B_6O_6) cluster[27] was shown to possess a robust boroxol ring already, rendering it an analogue of benzene and boroxine. Between the lower and upper bounds, we performed combined experimental and computational studies on the $B_4O_3^{-/0}$ and $B_4O_4^{-/0}$ clusters,[11,29] which are either open structures or possess a rhombic B_2O_2 ring. The present $B_4O_4^+$ (**1**, C_s, $^2A'$) cluster thus marks the exact onset of the boroxol ring in boron oxides, which represents the smallest boron oxide species with a boroxol ring. We stress that the genesis of the boroxol ring in $B_4O_4^+$ is governed by both geometric and electronic reasons; see Sections 4.2 and 4.3.

4.2. Double (π and σ) aromaticity: C_s $B_4O_4^+$ *versus* D_{3h} $C_6H_3^+$

The **1** (C_s, $^2A'$) global-minimum structure of the $B_4O_4^+$ cluster exhibits perfectly planar, annular shape, whose six-membered boroxol ring is known to possess a π sextet,[27] akin to benzene and boroxine. To understand the bonding nature of $B_4O_4^+$ (**1**, C_s, $^2A'$), we performed detailed CMO and AdNDP[33] analyses. Key CMOs relevant to the delocalized bonding in the B_3O_3 ring of **1** are shown in Fig. 3(a). The combination of HOMO−5 (HOMO denotes the highest occupied molecular orbital), HOMO−7, and HOMO−9 constitutes a delocalized 6π system, which is typical for complexes containing a boroxol ring,[27] rendering π aromaticity for **1** according to the ($4n$ + 2) Hückel rule. This 6π system originates from three O 2p lone-pairs, with the O6, O7, and O8 atoms each contributing one.[46] The AdNDP data fully recover the 6π system (Fig. 4(a); third row), which is presented as three three-center two-electron (3c–2e) BOB bonds, that is, the Kekulé structure. Note that the six B–O

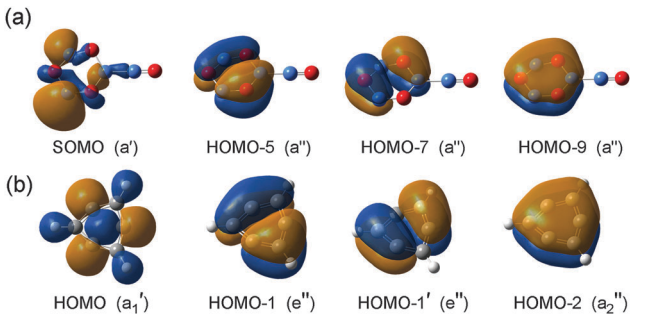

Fig. 3 Comparison of the delocalized π and σ canonical molecular orbitals (CMOs) of (a) C_s $B_4O_4^+$ (**1**) and (b) D_{3h} $C_6H_3^+$. SOMO stands for the single occupied molecular orbital.

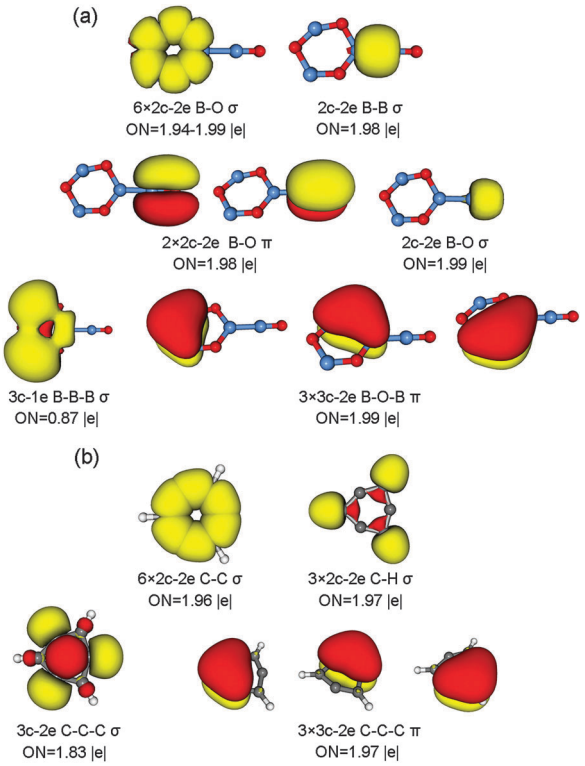

Fig. 4 The AdNDP bonding patterns for (a) $B_4O_4^+$ (**1**) and (b) $C_6H_3^+$. The four O 2*s* lone pairs in **1** are not depicted. The occupation numbers (ONs) are shown.

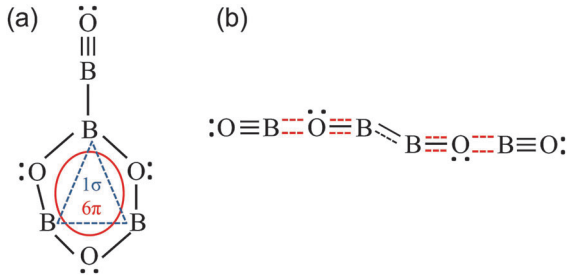

Fig. 5 Schematic Lewis presentations of (a) the hexagonal C_s (**1**) global minimum and (b) the quasi-linear C_{2h} isomer of $B_4O_4^+$. The delocalized bonding in (a) features a π sextet (in red) and a 3c–1e σ bond (in blue; dashed lines), rendering double aromaticity in **1**. The quasi-linear isomer (b) possesses dual 3c–4e B–O–B π bonds, shown as dashed lines in red, where a dashed line corresponds effectively to a bond order of 0.5.

σ bonds in the ring, the B–B σ bond, and the terminal B≡O triple bond are also recovered in the AdNDP results, as anticipated (Fig. 4(a); the first and second rows).

It is interesting to note the singly occupied molecular orbital (SOMO; Fig. 3(a)) of **1**. This is a σ CMO, being composed of B 2*s*/2*p* atomic orbitals (AOs) from B3, B4, and B1. While the contributions of the three B centers are not even, the SOMO is truly 3c–1e in nature, which is completely bonding. In the AdNDP analysis, the 3c–1e σ bond is also fully recovered (Fig. 4(a); third row). A delocalized 3c–1e σ bond is known to be σ aromatic, similar to a delocalized 3c–2e σ system, which follows the $(4n + 2)$ Hückel rule for σ aromaticity. Thus, **1** (C_s, $^2A'$) may be classified to be σ aromatic. Note that the 3c–1e σ bond is only half-occupied, which is relatively weak due to the large BB distances in the boroxol ring. To be specific, the B3B4 distance is 2.176 Å, which is far beyond the recommended upper limit for a B–B single bond (1.70 Å).[41] Consequently, the resonance stabilization of σ aromaticity in **1** is only half with respect to a 3c–2e σ aromatic system. This explains, at least partially, why structure **1** as the global minimum of the $B_4O_4^+$ cationic system adopts a distorted C_s structure, rather than C_{2v}.

The delocalized π and σ frameworks of **1** (Fig. 3(a) and 4(a)) collectively define a doubly (π and σ) aromatic system, whose approximate Lewis presentation is illustrated in Fig. 5(a). To the best of our knowledge, σ aromaticity has not been discussed for binary BO ring molecular systems to date. Double (π and σ) aromaticity in boron oxides has remained unknown in the literature. The $B_4O_4^+$ (**1**, C_s, $^2A'$) cluster is thus a unique species. It must be stressed that chemical bonding in boron oxides involves the close interplay of robust B≡O triple bonds *versus* B–O/B=O bonds, localized *versus* delocalized bonding, cyclic *versus* open structures, rhombic *versus* hexagonal rings, *etc.* For such electron-deficient systems, it is rather challenging to simultaneously reach the ideal B/O atomic ratio as well as the correct electron counting. The only way toward the discovery of a double aromatic boron oxide species is to systematically tune the cluster size, the B/O ratio, and the charge state. In this process, every B/O atom makes a difference and every electron counts.

Double (π and σ) aromaticity in $B_4O_4^+$ (**1**, C_s, $^2A'$) is immediate reminiscent of the 3,5-dehydrophenyl cation molecule, $C_6H_3^+$ (D_{3h}, $^1A_1'$) (Fig. 1(b)).[34] The latter species is often quoted as one of the milestone studies in the development of aromaticity concept *via* computational design. Indeed, the delocalized π and σ CMOs of $C_6H_3^+$ (Fig. 3(b)) show one-to-one correspondence to those of $B_4O_4^+$ (**1**, C_s, $^2A'$), except that the σ CMO in **1** is distorted due to its C_s symmetry. This similarity in the bonding pattern suggests that the $B_4O_4^+$ (**1**, C_s, $^2A'$) cluster is a boron oxide analogue of the 3,5-dehydrophenyl cation. The AdNDP data also support the remarkable analogy between the two species (Fig. 4), whose π systems are both illustrated as the Kekulé structures. It is important to note that the structural distortion of $B_4O_4^+$ (**1**) to C_s symmetry results in shortened B4O6/B4O8 (1.28 Å) *versus* elongated B1O8/B3O6 (1.46 Å) bonds. The former distance is close to a B=O bond,[2,41] which reflects the collective effects of the localized 2c–2e B–O σ bond, as well as the delocalized π sextet and the 3c–1e σ bond. The unevenness in bond distances is an indication that the π sextet is not uniformly distributed in the B_3O_3 ring, but it not necessarily suggests a localized 2c–2e π bond in B4O6 or B4O8.

The isolobal analogy between $B_4O_4^+$ (**1**) and $C_6H_3^+$ can also be revealed from a simple valence electron counting in the B_3O_3 *versus* C_6 hexagonal rings (Fig. 1). The C_6 ring in $C_6H_3^+$ has 23 valence electrons including the positive charge; the latter is distributed on the C2/C4/C6 centers. Three of these electrons are used for the C–H bonds, resulting in 20 electrons for bonding within the C_6 ring. Of these, 12 form the six C–C

2e–2e σ bonds. The remaining 8 electrons are responsible for global delocalized bonding (6π plus 2σ; Fig. 3(b)). Here every C center contributes one electron to the π sextet. Similarly, the B_3O_3 ring in $B_4O_4^+$ (**1**) has 20 valence electrons, where the positive charge is counted and three O 2s lone-pairs are not counted. Of these, one B center uses an electron for the terminal B–(BO) single bond and all B centers use six electrons in total for the six B–O 2e–2e σ bonds, whereas the three O centers provide the remaining six electrons for the latter bonds. Thus only seven electrons are left for global, delocalized bonding in the B_3O_3 ring: six electrons from the O centers form the π sextet and the single electron from the B centers makes the 3c–1e σ bond.

Note that the terminal BO group in $B_4O_4^+$ (**1**) is isolobal to an H terminal in $C_6H_3^+$, because both are monovalent σ radicals. The difference between the B_3O_3 and C_6 hexagonal rings is that the C1/C3/C5 centers in the latter, which form terminal C–H bonds (Fig. 1(b)), are relatively electron poor and thus do not participate in σ aromaticity. In contrast, the B centers in $B_4O_4^+$ (**1**), one of which also has a terminal ligand (Fig. 1(a)), manage to reserve one electron for the 3c–1e σ bond, despite the fact that the O centers have more valence electrons. This is because the O centers are solely responsible for the π sextet, with the B centers only offering the corresponding AOs and not the electrons. Therefore, in terms of the bonding analogy, the B1/B3/B4 centers in $B_4O_4^+$ (**1**) (Fig. 1(a)) should correspond to the C6/C2/C4 centers in $C_6H_3^+$ (Fig. 1(b)). The former centers in $B_4O_4^+$ (**1**) have relatively fewer valence electrons and are associated with a terminal BO group, whereas the latter centers in $C_6H_3^+$ are relatively electron-rich and do not bind to the H terminals. The above correspondence is exactly reflected in the orientation of the delocalized π and σ CMOs, as depicted in Fig. 3.

Double aromaticity in $B_4O_4^+$ (**1**, C_s, $^2A'$) may be further characterized using the nucleus-independent chemical shift (NICS). The calculated NICS values at the B3LYP level at the hexagon ''center'' and at 1 Å above it are NICS(0) = −5.6 ppm and NICS(1) = −3.4 ppm, where the ''center'' is defined as the arithmetic mean of Cartesian coordinates of the six B/O atoms in the hexagonal ring. Both of the NICS values are negative, confirming that **1** indeed possesses (π and σ) double aromaticity. For comparison, those calculated at the same level for D_{3h} $C_6H_3^+$ are NICS(0) = −43.8 ppm and NICS(1) = −19.7 ppm. It is stressed that boron oxide clusters always have weaker aromaticity with respect to typical hydrocarbons, because the π aromaticity in the former species originates from O 2p lone-pairs, whose extent of delocalization is relatively poor.[47] For instance, a recent report gives a NICS value of −3.4 ppm for the prototypical ''inorganic benzene'', boroxine $B_3O_3H_3$, at the B3LYP level, which is in contrast to −29.7 ppm for benzene.[27]

One reviewer suggests an interesting possibility of exploring similar bonding phenomena in the relevant Si–O systems or in clusters with CO ligands. While this is clearly beyond the scope of the current work, we would like to comment here that it is doable through careful computational design, by tuning the size, composition, and charge state. Nonetheless, considering the large difference in electronegativity between Si and O, 1.90 for Si *versus* 3.44 for O at the Pauling scale, the electrons (both π and σ) can be far more difficult to delocalize in a Si–O ring. Aromaticity in such molecules should thus be rather weak.

4.3. $B_4O_4^{+/0/-}$: dependence of conformation on the charge state

Very recently, we reported the global-minimum structures of $B_4O_4^-$ and B_4O_4 clusters *via* anion PES experiments, global structural searches, and electronic structure calculations.[29] As shown in Fig. 6(b), the global-minimum structures of $B_4O_4^{+/0/-}$ are distinctly different: hexagonal $B_4O_4^+$ (**1**, C_s, $^2A'$), rhombic B_4O_4 (**4**, D_{2h}, ^1A_g), and Y-shaped $B_4O_4^-$ (**7**, C_s, $^2A''$). All three types of conformation for three charge states (cation, neutral, and anion) were optimized herein at the B3LYP/aug-cc-pVTZ level, and the relative energies for the nine structures are shown in Fig. 6(b). The relative energies were also refined at the single-point CCSD(T) level. Notably, the stability for a specific conformation is sensitively charge-state dependent. For example, the hexagonal isomer is the global minimum for $B_4O_4^+$ (**1**); whereas it becomes the least stable of the three for B_4O_4 (**6**) or $B_4O_4^-$ (**9**), being 34 and 55 kcal mol^{-1} above the global minimum at the CCSD(T) level, respectively. The Y-shaped isomer is 82 kcal mol^{-1} above the global minimum for $B_4O_4^+$ (**3**). However, it gradually gains stability with the addition of extra electrons, which is only 18 kcal mol^{-1} above the global minimum for B_4O_4 (**5**) and further becomes the global minimum for $B_4O_4^-$ (**7**).

To be quantitative, going from $B_4O_4^+$ to B_4O_4 (Fig. 6(b)), the rhombic and Y-shaped isomers gain an enhanced stability of 122 kcal mol^{-1} (**2** → **4**) and 98 kcal mol^{-1} (**3** → **5**) with respect to the hexagonal isomer (**1** → **6**). Similarly, going from B_4O_4 to $B_4O_4^-$, the Y-shaped isomers gain an enhanced stability of 26 kcal mol^{-1} (**5** → **7**) with respect to the rhombic isomer (**4** → **8**). The above enhancement of stability is remarkable, demonstrating an interesting electronic system in which a single electron can make a difference. This observation may be entirely attributed to boron's intrinsic electron-deficiency.

As an alternative presentation, the dependence of conformation on the charge state in the $B_4O_4^{+/0/-}$ series can be rationalized using the ionization potentials (IPs) and electron affinities (EAs) for the three isomeric structures of B_4O_4 (**4–6**; Fig. 6(a)), which are calculated at both the B3LYP/aug-cc-pVTZ and single-point CCSD(T) levels. The IP of the hexagonal isomer B_4O_4 (**6**) is 8.46 eV at CCSD(T), being substantially lower than those of the rhombic and Y-shaped isomers (13.75 eV for **4**; 12.70 eV for **5**). The extremely low IP of **6** manages to gain an enhanced stability of 4.2–5.3 eV for the hexagonal isomer in the cationic charge state, which offsets the relative energy of **6** with respect to **4**/**5**. This explains why **1** becomes the global minimum for $B_4O_4^+$. On the other hand, Y-shaped **5** possesses a much higher EA (2.57 eV) than other isomers (1.43 eV for **4**; 0.89 eV for **6**), which makes the Y-shaped isomer (**7**) the global minimum for the anion. The low EA of hexagonal isomer **6** further reinforces the instability of hexagonal isomer **9** as an anion.

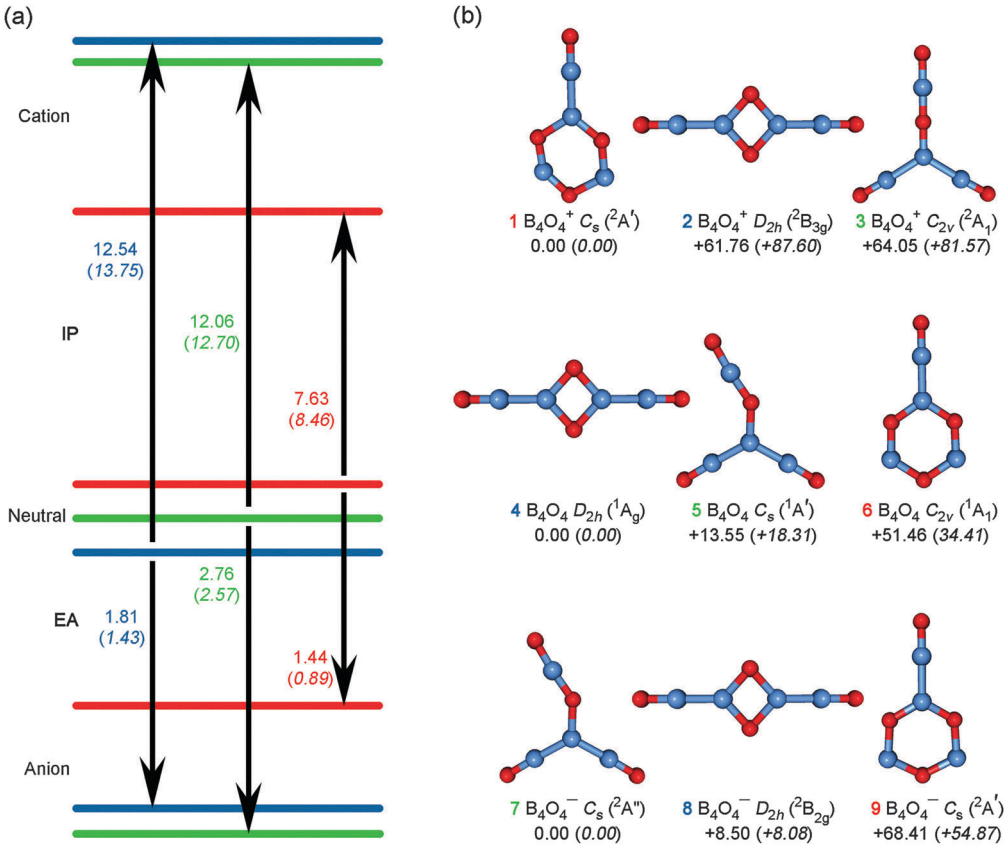

Fig. 6 (a) Schematic diagram (not to scale) showing the relative energies of three isomeric structures in three charge states. The calculated ionization potentials (IPs) and electron affinities (EAs) are shown in eV at the B3LYP and single-point CCSD(T) (in parentheses) levels. (b) Structures of **1–9** and their relative energies (in kcal mol^{-1}) at the B3LYP and single-point CCSD(T) (in parentheses) levels. The B atom is in blue and O is in red.

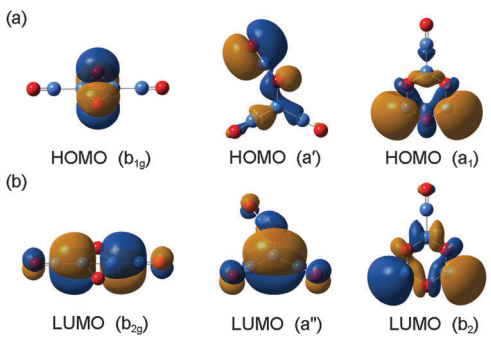

Fig. 7 Pictures of (a) the highest occupied molecular orbitals (HOMOs) and (b) the lowest unoccupied molecular orbitals (LUMOs) for the three typical isomeric structures of B_4O_4 (**4–6**). These orbitals hold the key to understanding the structural evolution of $B_4O_4^{+/0/-}$ with charge states (Fig. 6).

Not surprisingly, the calculated IP and EA values are closely related to the nature of the frontier CMOs of **4–6** (Fig. 7). The HOMOs (Fig. 7(a)) determine the IPs of **4–6**. It is nonbonding based on O 2p AOs for **4**, BO π bonding for **5**, and B based for **6**, consistent with their decreasing IP values. In particular, the IP value drops sharply from **4**/**5** to **6**. For the lowest unoccupied molecular orbitals (LUMOs; Fig. 7(b)), it is π bonding based on all B centers but with partial antibonding character for **4**, completely π bonding based on three B centers for **5**, and B based σ CMO with antibonding character for **6**, which are consistent with the fact that **5** has the highest EA and **6** has the lowest. In summary, the IPs and EAs of the three neutral conformers (**4–6**) appear to hold the key to the structural changes along the $B_4O_4^{+/0/-}$ series.

It is interesting to comment here that, despite its bonding nature of double aromaticity, the hexagonal structure is the global minimum for the $B_4O_4^+$ (**1**) cationic cluster only (Fig. 6). With one or two extra electrons being added to the system, the rhombic or Y-shaped structures are more favorable, because the extra electrons enter distinctly different orbitals in different isomers (Fig. 7). Thus the doubly aromatic $B_4O_4^+$ (**1**) cluster as the global minimum is a delicate balance of the B/O atomic ratio, atomic connectivity, and electron counting. In this respect, "aromaticity" does not necessarily dominate the stability of the system.

4.4. On the "speculative" structure of 1988: quasi-linear C_{2h} $B_4O_4^+$

One of the motivations of this computational study on the $B_4O_4^+$ cluster comes from the 1988 experimental work by Doyle,[30] who examined a variety of $B_mO_n^+$ using the CID technique. The collisional activation spectrum of the $B_4O_4^+$ cluster deviates from the general trend of $B_mO_n^+$ dissociation,

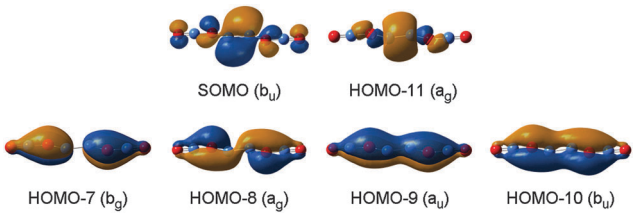

Fig. 8 Selected canonical molecular orbitals (CMOs) of the quasi-linear $B_4O_4^+$ C_{2h} (^2B_u) isomer. SOMO stands for the single occupied molecular orbital.

suggesting the presence of a BB bond in $B_4O_4^+$. Doyle thus proposed a "speculative" linear structure for $B_4O_4^+$ (Scheme 1). Our current study appears to be the first to systematically examine the potential energy surface of $B_4O_4^+$ *via* global structural searches (Fig. 2). The quasi-linear C_{2h} (^2B_u) structure (Fig. 1(c)) should best match that proposed by Doyle, although their bonding details differ markedly. The C_{2h} (^2B_u) structure turns out to be $\sim$29 kcal mol^{-1} above the global minimum at the single-point CCSD(T) level (Fig. 2), which was thus unlikely to be present in the 1988 experiments.

Despite its high energetics, chemical bonding in the quasi-linear $B_4O_4^+$ C_{2h} (^2B_u) structure remains interesting. Fig. 8 shows a few key CMOs. HOMO−11 is the B–B σ bond, whereas the π SOMO is also primarily responsible for the B–B bonding. These collectively define a B–B bond with a formal order of 1.5, consistent with the relatively short distance of 1.59 Å, which fall between typical B–B and B═B bonds.[12,41] HOMO−9/HOMO−7 represents a pair of 3c–2e B–O–B π bonds (B2–O7–B3 and B4–O8–B1). Similarly, HOMO−10/HOMO−8 represents another pair of 3c–2e B–O–B π bonds. Other CMOs are shown in Fig. S2 in the ESI.† Overall, the bonding in C_{2h} (^2B_u) can be summarized as the Lewis presentation, which suggests that the B2O5, B2O7, and B3O7 bonds have very different bond orders (that is, effectively three, one, and two, respectively; Fig. 5(b)), consistent with their bond distances of 1.19, 1.35, and 1.26 Å.[2,41] We stress that this Lewis presentation differs markedly from the 1988 proposal (Scheme 1).[30]

Based on the current data, it is imperative that we reinterpret the experimental CID data using the global-minimum structure: $B_4O_4^+$ (**1**, C_s, $^2A'$). The observed CID products of $B_4O_4^+$ are $B_2O_2^+$ (loss of B_2O_2) and $B_3O_3^+$ (loss of BO).[30] In **1** (C_s, $^2A'$), the positive charge is located on the B4 and B3 centers, in particular on B4 (Fig. 1(a) and Fig. S3(a) in the ESI†). The cleavage of B1O8 and B3O7 bonds will produce $B_2O_2^+$ with the loss of B_2O_2, whereas the cleavage of the B1B2 bond will produce $B_3O_3^+$ with the loss of BO. These are the possible dissociation channels observed. Interestingly, the latter channel hints that a hexagonal $B_3O_3^+$ ring might be accessible as a CID product, although the gas-phase $B_3O_3^+$ cluster possesses a linear global-minimum structure.[26]

5. Conclusions

In this paper, we report on the first-principles theoretical prediction of the global-minimum structure of the boron oxide $B_4O_4^+$ cluster. The calculations include extensive Coalescence Kick structural searches, electronic structural calculations at the B3LYP and single-point CCSD(T) levels, and chemical bonding analyses. The $B_4O_4^+$ cationic cluster is shown to possess a perfectly planar, hexagonal (C_s, $^2A'$) structure as the global minimum, which contains a boroxol B_3O_3 ring and a terminal boronyl group. It marks the exact onset of the boroxol ring in boron oxide clusters. Chemical bonding analyses show that $B_4O_4^+$ (C_s, $^2A'$) features double (π and σ) aromaticity, rendering it an interesting boron oxide analogue of the 3,5-dehydrophenyl cation. The hexagonal (C_s, $^2A'$) global-minimum structure of $B_4O_4^+$ differs marked from a "speculative" linear structure proposed in 1988, as well as from the recently established rhombic and Y-shaped global minima for B_4O_4 and $B_4O_4^-$, respectively. The $B_4O_4^{+/0/-}$ series represent a unique molecular system, in which a single electron can make a difference. The $B_4O_4^+$ (C_s, $^2A'$) global-minimum structure also helps reinterpret the experimental collisional activation spectrum in the literature.

Acknowledgements

This work was supported by the National Natural Science Foundation of China (21573138) and in part by the State Key Laboratory of Quantum Optics and Quantum Optics Devices (KF201402). H.J.Z. gratefully acknowledges the start-up fund from Shanxi University for support.

References

1 S. H. Bauer, *Chem. Rev.*, 1996, **96**, 1907.
2 H. J. Zhai, Q. Chen, H. Bai, S. D. Li and L. S. Wang, *Acc. Chem. Res.*, 2014, **47**, 2435.
3 P. G. Wenthold, J. B. Kim, K. L. Jonas and W. C. Lineberger, *J. Phys. Chem. A*, 1997, **101**, 4472.
4 H. J. Zhai, L. M. Wang, S. D. Li and L. S. Wang, *J. Phys. Chem. A*, 2007, **111**, 1030.
5 D. Yu. Zubarev, A. I. Boldyrev, J. Li, H. J. Zhai and L. S. Wang, *J. Phys. Chem. A*, 2007, **111**, 1648.
6 H. Bai, H. J. Zhai, S. D. Li and L. S. Wang, *Phys. Chem. Chem. Phys.*, 2013, **15**, 9646.
7 H. Bock, L. Cederbaum, W. von Niessen, P. Paetzold, P. Rosmus and B. Solouki, *Angew. Chem., Int. Ed. Engl.*, 1989, **28**, 88.
8 M. L. Drummond, V. Meunier and B. G. Sumpter, *J. Phys. Chem. A*, 2007, **111**, 6539.
9 (*a*) T. B. Tai and M. T. Nguyen, *Chem. Phys. Lett.*, 2009, **483**, 35; (*b*) M. T. Nguyen, M. H. Matus, V. T. Ngan, D. J. Grant and D. A. Dixon, *J. Phys. Chem. A*, 2009, **113**, 4895; (*c*) T. B. Tai, M. T. Nguyen and D. A. Dixon, *J. Phys. Chem. A*, 2010, **114**, 2893.
10 C. B. Shao, L. Jin and Y. H. Ding, *J. Comput. Chem.*, 2011, **32**, 771.
11 H. J. Zhai, S. D. Li and L. S. Wang, *J. Am. Chem. Soc.*, 2007, **129**, 9254.
12 S. D. Li, H. J. Zhai and L. S. Wang, *J. Am. Chem. Soc.*, 2008, **130**, 2573.

13 (*a*) H. J. Zhai, J. C. Guo, S. D. Li and L. S. Wang, *ChemPhysChem*, 2011, **12**, 2549; (*b*) H. Bai, H. J. Zhai, S. D. Li and L. S. Wang, *Phys. Chem. Chem. Phys.*, 2013, **15**, 9646; (*c*) Q. Chen, H. J. Zhai, S. D. Li and L. S. Wang, *J. Chem. Phys.*, 2012, **137**, 044307; (*d*) Q. Chen, H. Bai, H. J. Zhai, S. D. Li and L. S. Wang, *J. Chem. Phys.*, 2013, **139**, 044308; (*e*) H. J. Zhai, C. Q. Miao, S. D. Li and L. S. Wang, *J. Phys. Chem. A*, 2010, **114**, 12155; (*f*) W. Z. Yao, J. C. Guo, H. G. Lu and S. D. Li, *J. Phys. Chem. A*, 2009, **113**, 2561; (*g*) H. J. Zhai, Q. Chen, H. Bai, H. G. Lu, W. L. Li, S. D. Li and L. S. Wang, *J. Chem. Phys.*, 2013, **139**, 174301; (*h*) D. Z. Li, L. J. Zhang, T. Ou, H. X. Zhang, L. Pei, H. J. Zhai and S. D. Li, *Phys. Chem. Chem. Phys.*, 2015, **17**, 16798; (*i*) W. J. Tian, H. G. Xu, X. Y. Kong, Q. Chen, W. J. Zheng, H. J. Zhai and S. D. Li, *Phys. Chem. Chem. Phys.*, 2014, **16**, 5129.

14 (*a*) H. J. Zhai, L. S. Wang, A. N. Alexandrova and A. I. Boldyrev, *J. Phys. Chem. A*, 2003, **107**, 9319; (*b*) A. N. Alexandrova, A. I. Boldyrev, H. J. Zhai, L. S. Wang, E. Steiner and P. W. Fowler, *J. Phys. Chem. A*, 2003, **107**, 1359; (*c*) A. N. Alexandrova, A. I. Boldyrev, H. J. Zhai and L. S. Wang, *J. Phys. Chem. A*, 2004, **108**, 3509; (*d*) H. J. Zhai, A. N. Alexandrova, K. A. Birch, A. I. Boldyrev and L. S. Wang, *Angew. Chem., Int. Ed.*, 2003, **42**, 6004; (*e*) A. N. Alexandrova, H. J. Zhai, L. S. Wang and A. I. Boldyrev, *Inorg. Chem.*, 2004, **43**, 3552.

15 (*a*) A. P. Sergeeva, D. Yu. Zubarev, H. J. Zhai, A. I. Boldyrev and L. S. Wang, *J. Am. Chem. Soc.*, 2008, **130**, 7244; (*b*) C. Romanescu, D. J. Harding, A. Fielicke and L. S. Wang, *J. Chem. Phys.*, 2012, **137**, 014317.

16 A. N. Alexandrova, A. I. Boldyrev, H. J. Zhai and L. S. Wang, *Coord. Chem. Rev.*, 2006, **250**, 2811.

17 (*a*) B. Kiran, S. Bulusu, H. J. Zhai, S. Yoo, X. C. Zeng and L. S. Wang, *Proc. Natl. Acad. Sci. U. S. A.*, 2005, **102**, 961; (*b*) Z. A. Piazza, W. L. Li, C. Romanescu, A. P. Sergeeva, L. S. Wang and A. I. Boldyrev, *J. Chem. Phys.*, 2012, **136**, 104310; (*c*) A. P. Sergeeva, Z. A. Piazza, C. Romanescu, W. L. Li, A. I. Boldyrev and L. S. Wang, *J. Am. Chem. Soc.*, 2012, **134**, 18065; (*d*) I. A. Popov, Z. A. Piazza, W. L. Li, L. S. Wang and A. I. Boldyrev, *J. Chem. Phys.*, 2013, **139**, 144307; (*e*) Z. A. Piazza, I. A. Popov, W. L. Li, R. Pal, X. C. Zeng, A. I. Boldyrev and L. S. Wang, *J. Chem. Phys.*, 2014, **141**, 034303.

18 (*a*) W. L. Li, Y. F. Zhao, H. S. Hu, J. Li and L. S. Wang, *Angew. Chem., Int. Ed.*, 2014, **53**, 5540; (*b*) W. L. Li, Q. Chen, W. J. Tian, H. Bai, Y. F. Zhao, H. S. Hu, J. Li, H. J. Zhai, S. D. Li and L. S. Wang, *J. Am. Chem. Soc.*, 2014, **136**, 12257; (*c*) Z. A. Piazza, H. S. Hu, W. L. Li, Y. F. Zhao, J. Li and L. S. Wang, *Nat. Commun.*, 2014, **5**, 3113; (*d*) Q. Chen, G. F. Wei, W. J. Tian, H. Bai, Z. P. Liu, H. J. Zhai and S. D. Li, *Phys. Chem. Chem. Phys.*, 2014, **16**, 18282.

19 H. J. Zhai, Y. F. Zhao, W. L. Li, Q. Chen, H. Bai, H. S. Hu, Z. A. Piazza, W. J. Tian, H. G. Lu, Y. B. Wu, Y. W. Mu, G. F. Wei, Z. P. Liu, J. Li, S. D. Li and L. S. Wang, *Nat. Chem.*, 2014, **6**, 727.

20 H. J. Zhai, B. Kiran, J. Li and L. S. Wang, *Nat. Mater.*, 2003, **2**, 827.

21 W. Huang, A. P. Sergeeva, H. J. Zhai, B. B. Averkiev, L. S. Wang and A. I. Boldyrev, *Nat. Chem.*, 2010, **2**, 202.

22 J. E. Fowler and J. M. Ugalde, *J. Phys. Chem. A*, 2000, **104**, 397.

23 J. I. Aihara, H. Kanno and T. Ishida, *J. Am. Chem. Soc.*, 2005, **127**, 13324.

24 Q. Chen, W. L. Li, Y. F. Zhao, S. Y. Zhang, H. S. Hu, H. Bai, H. R. Li, W. J. Tian, H. G. Lu, H. J. Zhai, S. D. Li, J. Li and L. S. Wang, *ACS Nano*, 2015, **9**, 754.

25 Q. Chen, S. Y. Zhang, H. Bai, W. J. Tian, T. Gao, H. R. Li, C. Q. Miao, Y. W. Mu, H. G. Lu, H. J. Zhai and S. D. Li, *Angew. Chem., Int. Ed.*, 2015, **54**, 8160.

26 Q. Chen, H. G. Lu, H. J. Zhai and S. D. Li, *Phys. Chem. Chem. Phys.*, 2014, **16**, 7274.

27 D. Z. Li, H. Bai, Q. Chen, H. G. Lu, H. J. Zhai and S. D. Li, *J. Chem. Phys.*, 2013, **138**, 244304.

28 W. Wang, Q. Chen, Y. J. Wang, H. Bai, T. T. Gao, H. R. Li, H. J. Zhai and S. D. Li, *Phys. Chem. Chem. Phys.*, 2015, **17**, 19929.

29 W. J. Tian, L. J. Zhao, Q. Chen, T. Ou, H. G. Xu, W. J. Zheng, H. J. Zhai and S. D. Li, *J. Chem. Phys.*, 2015, **142**, 134305.

30 R. J. Doyle, Jr., *J. Am. Chem. Soc.*, 1988, **110**, 4120.

31 A. P. Sergeeva, B. B. Averkiev, H. J. Zhai, A. I. Boldyrev and L. S. Wang, *J. Chem. Phys.*, 2011, **134**, 224304.

32 (*a*) M. Saunders, *J. Comput. Chem.*, 2004, **25**, 621; (*b*) P. P. Bera, K. W. Sattelmeyer, M. Saunders and P. v. R. Schleyer, *J. Phys. Chem. A*, 2006, **110**, 4287.

33 D. Yu. Zubarev and A. I. Boldyrev, *Phys. Chem. Chem. Phys.*, 2008, **10**, 5207.

34 (*a*) J. Chandrasekhar, E. D. Jemmis and P. v. R. Schleyer, *Tetrahedron Lett.*, 1979, **20**, 3707; (*b*) P. v. R. Schleyer, H. J. Jiao and M. N. Glukhovtsev, *J. Am. Chem. Soc.*, 1994, **116**, 10129.

35 R. A. Kendall, T. H. Dunning, Jr. and R. J. Harrison, *J. Chem. Phys.*, 1992, **96**, 6796.

36 J. Čížek, *Adv. Chem. Phys.*, 1969, **14**, 35.

37 G. E. Scuseria and H. F. Schaefer III, *J. Chem. Phys.*, 1989, **90**, 3700.

38 R. J. Bartlett and M. Musial, *Rev. Mod. Phys.*, 2007, **79**, 291.

39 E. D. Glendening, J. K. Badenhoop, A. E. Reed, J. E. Carpenter, J. A. Bohmann, C. M. Morales and F. Weinhold, *NBO 5.0*, Theoretical Chemistry Institute, University of Wisconsin, Madison, 2001.

40 M. J. Frisch, *et al.*, *GAUSSIAN 09, Revision D.01*, Gaussian, Inc., Wallingford, CT, 2009.

41 (*a*) P. Pyykkö and M. Atsumi, *Chem. – Eur. J.*, 2009, **15**, 12770; (*b*) P. Pyykkö, *J. Phys. Chem. A*, 2015, **119**, 2326.

42 A. Moezzi, R. A. Bartlett and P. P. Power, *Angew. Chem., Int. Ed. Engl.*, 1992, **31**, 1082.

43 A. Moezzi, M. M. Olmstead and P. P. Power, *J. Am. Chem. Soc.*, 1992, **114**, 2715.

44 G. Ferlat, T. Charpentier, A. P. Seitsonen, A. Takada, M. Lazzeri, L. Cormier, G. Calas and F. Mauri, *Phys. Rev. Lett.*, 2008, **101**, 065504.

45 J. D. Mackenzie, *J. Phys. Chem.*, 1959, **63**, 1875.

46 The nature that the π sextet in $B_4O_4^+$ (**1**) originates from three O 2p lone-pairs is easily understandable. The B1/B3/B4 centers only have 8 valence electrons after taking into account the extra positive charge. Of these, one is used for the terminal B–(BO) σ bond and six participate in the six 2c–2e B–O σ bonds. The remaining one forms the delocalized 3c–1e σ bond and renders σ aromaticity for the system. Thus, the B1/B3/B4 centers cannot afford even a single electron for the π sextet. Indeed, orbital component analyses show that O 2p atomic orbitals (AOs) constitute 90%, 95%, and 72% of the delocalized HOMO−5, HOMO−7, and HOMO−9 orbitals, respectively (Fig. 3(a)). The AdNDP pattern also indicates the predominant role of O 2p AOs in the π sextet (Fig. 4(a)).

47 Despite the small NICS values in $B_4O_4^+$ (**1**), the π sextet appears to have a substantial bonding effect in terms of energetics. The completely bonding HOMO−9 (Fig. 3(a)) possesses an orbital energy that is 2.39 eV lower than HOMO−5, whereas HOMO−7 is only marginally lower than HOMO−5 by 0.11 eV. This pattern also indicates that the C_s distortion of $B_4O_4^+$ (**1**) results in a relative minor splitting of the HOMO−5/HOMO−7 orbitals.

